UNSYS digital

The Journal of Instrumentation, Automation and Systems

Design and Construction of a Magnetic Field Simulator for CubeSat Attitude Control Testing

Mark A. Post, Junquan Li, and Regina Lee

Department of Earth and Space Science and Engineering, York University, Ontario, Canada

Abstract—A real time, three-axis space magnetic field simulator, developed using only commercial, off-the-shelf components, is described in this paper. It is a complete and independent system to be used for the ground testing of nanosatellites, allowing automated magnetic attitude control systems to be verified. The main aim of this simulator is to reproduce magnetic field conditions in orbit with low cost mechanical and electronic designs. The system is capable of creating a region of uniform, directed magnetic field on command for nanosatellite ground testing.

Keywords—Nanosatellites, electromagnetism, Helmholtz coils, attitude control.

I. Introduction

Earth's magnetic field is constantly changing because it is generated by the motion of molten iron alloys in the Earth's outer core. The geomagnetic field also comes from the Earth's lithosphere. The Sun heats the ionosphere and generates a current flow, which causes diurnal fluctuations in the geomagnetic field. Coronal mass ejections or high velocity plasma from the Sun can cause magnetic storms. These storms have an 11-year solar cycle. There are several geomagnetic models that can be used to recreate this ever-changing magnetic field. The International Geomagnetic Reference Field (IGRF) model is the most used geomagnetic field model [1] despite neglecting ionospheric diurnal fluctuations and magnetospheric storms. The primary goal of this paper is to detail the replication of this field in the laboratory using inexpensive, commercially-available hardware.

Satellites and other spacecraft must make use of the Earth's magnetic field for sensing and attitude control purposes, but ground testing of satellite hardware requires that the magnetic conditions at a given point in Earth orbit must be replicated in the laboratory. One device capable of generating a uniform magnetic field is the Helmholtz coil, which consists of a pair of thin wire coils parallel to each other, with N complete turns of wire each. The configuration of three such coil pairs at orthogonal angles is known as a Helmholtz cage. The NASA Goddard Space Flight Center built a Braunbeck coil (a modified Helmholtz coil) system in 1960. However, the system was expensive and not suitable for testing of small research satellites. Commercial cages are also available (MacIntyre Electronic Design Associates and Astro-ind Feinwerktechnik Adlershof GmbH, [2] and [3]). Several universities (the Delft University of Technology, University of Michigan, Lulea University of Technology, University of Naples, and Air Force Institute of Technology) have all built Helmholtz cages to develop and test satellite attitude determination and control systems [4] [5] [6] [7] and [8]. There are several references regarding the design and construction of three axis space magnetic simulators [9] [10] and [11], and Helmholtz cages are also used to provide uniform magnetic fields for magnetic sensor calibration and validation [12].

While Helmholtz cages such as these have been in use for many different magnetic applications, there has not been much focus on a mechanical and electronic design that can be built and used by educational institutions specifically for nano-satellite programs. Limitations in the space, power, and complexity available to educational systems results in a different approach to design from proprietary industrial systems. Our approach is to maximize the flexibility and programmability of the magnetic field simulator while minimizing cost and complexity with the techniques detailed within this paper. To this end, we describe a mechanical design that is lightweight and easy to fabricate but adjustable, and an electronic design from commercial parts that is fully programmable and powerful. While complex control systems and linear current limiting often must be used on laboratory systems, we show that acceptable results can be achieved using more efficient filtered pulse-width modulation and serial communications to a single microcontroller from a host computer.

A CubeSat form factor nanosatellite with a three-axis magnetic attitude determination and control system (ADCS) is currently being developed at York University in Toronto, Canada. This satellite will carry a spectrometer to conduct atmospheric greenhouse gas research from Low Earth Orbit. Nanosatellites in Low Earth Orbit (LEO) usually use a passive or active magnetic system for attitude determination and control [13], and such magnetic attitude control systems are essential as they are more reliable, use less power, and are less costly than other control methods such as wheels or thrusters. The satellite includes a magnetometer, sun sensors, three magnetorquer rods, and one reaction wheel. Magnetometers are commonly used to estimate the satellite orientation with respect to the geomagnetic field. Ground testing of the Attitude Determination and Control Systems (ADCS) for a spacecraft

Corresponding author: Mark Andrew Post (e-mail: markpost@yorku.ca).
This paper was submitted on February 15, 2014; revised on May 20, 2014; and accepted on June 6, 2014.

includes numerical simulation, experimental testing, and hardware in the loop simulation [14] [15]. All the individual components on a satellite need to be experimentally checked before the launch. A B-dot controller and a nonlinear controller are used for detumbling mode and three-axis stabilization mode, respectively.

To test the B-dot and active magnetic controller designs on actual hardware, a Helmholtz cage has been purpose-built to simulate the space environment, and this paper focuses on the design and validation of this magnetic simulator system. As a research system developed under stringent time and budget limitations, the design and construction of the cage and controller was carried out completely within the university by Engineering students using commercial off-the-shelf hardware. A spherical air bearing system is used inside the Helmholtz cage to allow the ADCS hardware a full three axes of friction-free rotation. The Helmholtz cage and air bearing can be used to verify ADCS systems within 1U, 2U, or 3U CubeSat form factor nanosatellites, which share a similar configuration by design. The simulator is configured as an open loop system in which calibrated amounts of current are used to generate the in-orbit magnetic field, and also provides current, voltage, and magnetic field feedback that can be used for closed-loop control by a host computer.

The organization of this paper proceeds as follows: In Section II, the mathematical cage model is presented. In Section III, the mechanical design of the cage is shown, and Section IV provides the design of the control electronics. The question of field calibration is addressed in Section V. Lastly, testing of the field inside the cage is documented in Section VI to validate the performance of the magnetic field simulator.

II. Mathematical Model

Magnetic fields are produced by electric currents, which can be macroscopic currents in wires, or microscopic currents associated with electrons in atomic orbits. The magnetic field B is defined in terms of force on moving charge by the Lorentz force law. Finding the magnetic field resulting from a current distribution involves a vector product, and is inherently a calculus problem when the distance from the current to the field point is continuously changing.

$$dB = \mu_o \frac{I}{4\pi} \frac{d\vec{l} \times \vec{r}}{r^3} \tag{1}$$

Equation (1) computes the resultant magnetic field B at position r generated by a steady current I. $\vec{r}$ is the full displacement vector from the wire element to the point at which the field is being computed. μ_0 is the vacuum permeability. $d\vec{l}$ is a vector whose magnitude is the length of the differential element of the wire, in the direction of conventional current. In a pair of Helmholtz coils the magnetic field at the center of the coils is obtained by (2) [8]

$$B = \frac{4\mu_o NI}{\pi a(1+\gamma^2)\sqrt{2+\gamma^2}} \tag{2}$$

where N is the number of turns of wire in each coil, I is the current passing through the coils, a is half the length of the coils, and $\gamma$is the ratio of the distance between the two coils $2b$ and the length of the coils $2a$, such that $\gamma = 2\mathrm{b}/2\mathrm{a}$. The magnetic field generated by both coils in the vector along the coil axis (denoted as Z in coil coordinates) is given in (3) [9].

$$B_z = 2\frac{\mu_0}{\pi} IL^2 \left(\frac{\sqrt{Z^2 + dZ + \frac{d^2}{4} + \frac{L^2}{2}}}{4Z^2 + 4dZ + d^2 + L^2} + \frac{\sqrt{Z^2 dZ + \frac{d^2}{4} + \frac{L^2}{2}}}{4Z^2 - 4dZ + d^2 + L^2} \right) \tag{3}$$

At the latitude where the cage is located, the intensity of the Earth's magnetic field is about 51 μT and the maximum field strength required for simulation was estimated to be 20 μT. Therefore, with a margin of safety, a magnetic field strength of 100 μT is estimated as the minimum requirement for the cage. The magnetic field at the generic point P is obtained by integrating (1) along the coil, with L being the dimension of a square coil. The distance d between the coils is adjusted to obtain the largest homogeneous magnetic field volume. For the couple of the coils, the magnetic field generated at point P is the sum of the field vectors of both coils [9]. To achieve a uniform field at the center of the cage, the second derivative of $B_z$must be zero. The distance between the two coils to obtain a maximally uniform magnetic field in the center of the coils is $d = 0.5445\mathrm{L}$ [9] [10].

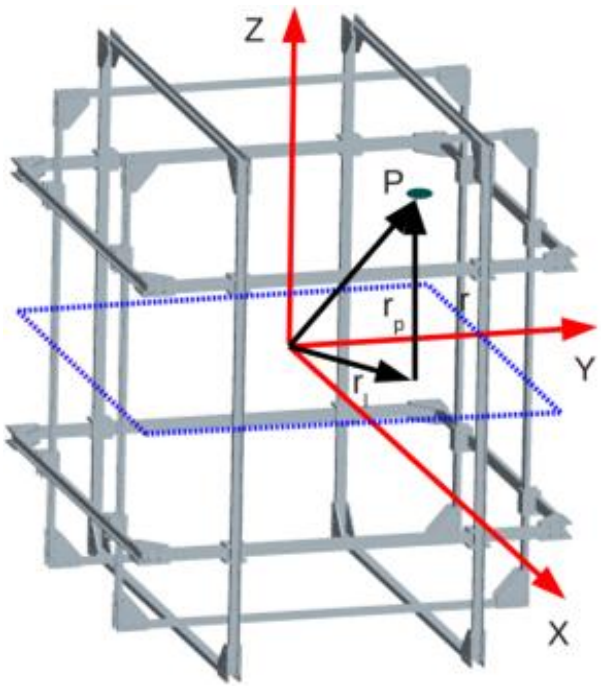

Figure 1 CAD model of Helmholtz cage and reference geometry

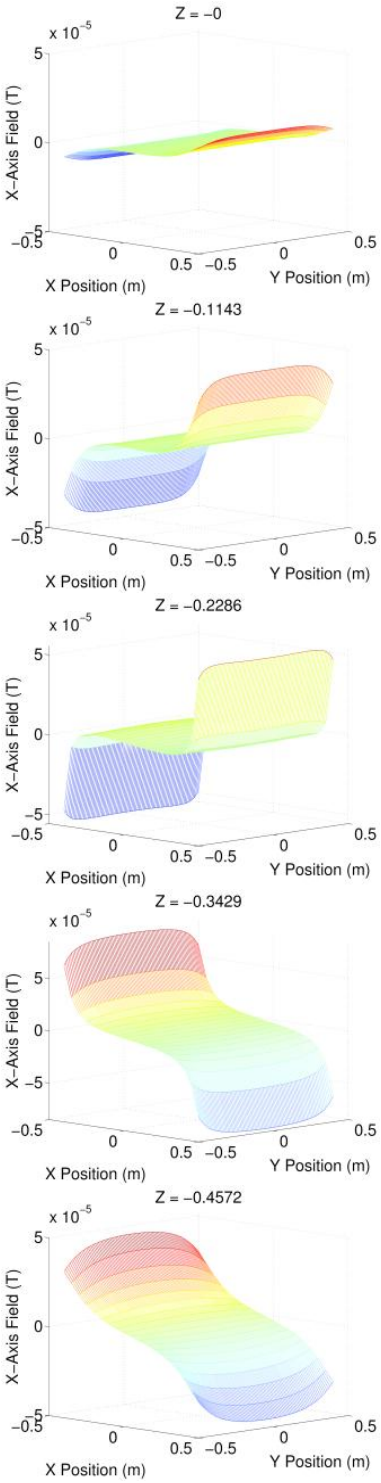

Figure 2 Calculated cage magnetic field strength in X direction for lower half-cage

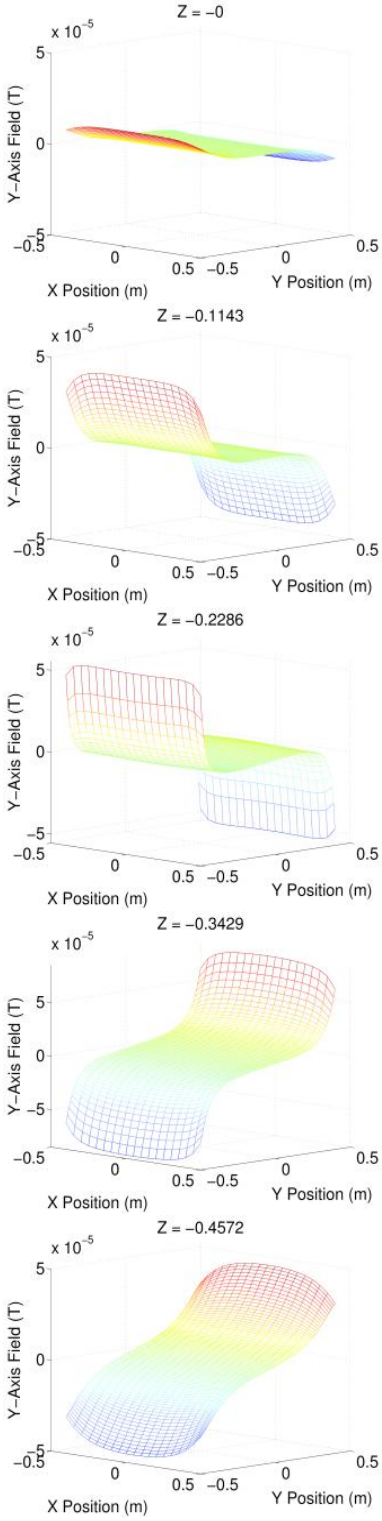

Figure 3 Calculated cage magnetic field strength in Y direction for lower half-cage

Using this calculation, a current of at least 1 A will be required to generate a magnetic field of approximately 51 μT with a sufficient safety margin, and 2 A will be needed for the safety margin of 100 μT. To create a uniform region at least 0.3 m in size so that a 3U CubeSat can be contained within it, a cage of approximately 1 m^3 volume will be required, as a 0.1 % maximum error is present in the central 30 % of the cage [16]. While the coils can be modeled as systems with characteristic reactance [17], the large size and relatively low number of turns combined with the low operating frequencies means that mutual inductance and capacitance values can be largely neglected in the driver design. A solid model with the geometric reference configuration used in this analysis is shown in **Figure 1**.

To evaluate the performance of the cage with respect to theoretical calculations, it is necessary to simulate the field generated by the cage in three dimensions for later comparison to measured values.

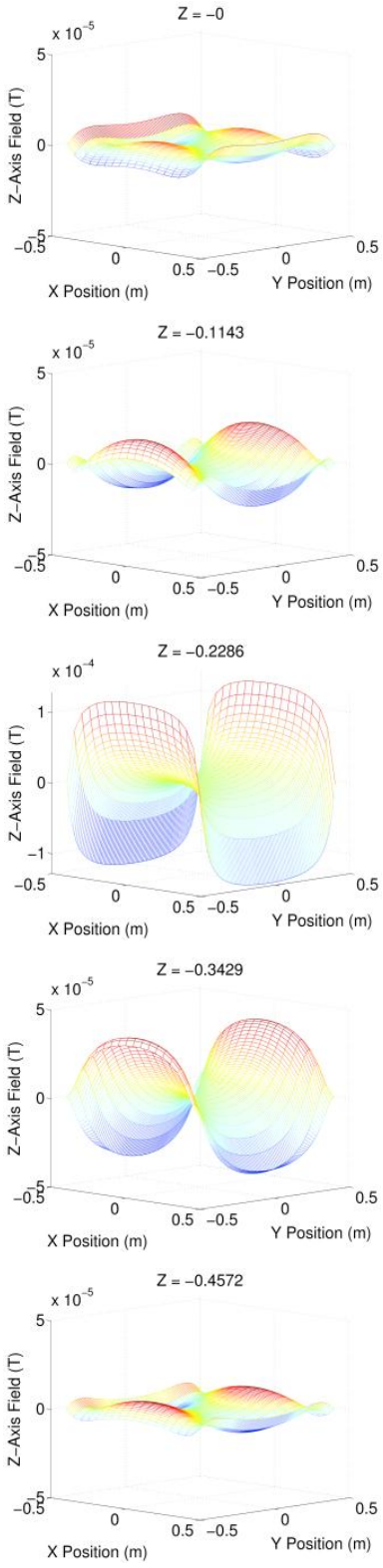

Figure 4 Calculated cage magnetic field strength in Z direction for lower half-cage

For simulation, a field along the cage *Z*-axis was simulated by assuming 1 A of current flowing through the *Z*-axis coils only, with the X-axis and Y-axis coils inactive, and calculating B_Z at a grid of points within the cage using (3). **Figure 2**, **Figure 3**, and **Figure 4** show the numerically calculated magnetic field vector component magnitudes B_X, B_Y, and B_Z respectively that are parallel to the the *X*, *Y*, and *Z* axes respectively. To illustrate as much of the three-dimensional field as possible, field strength in a given axis direction is shown as a series of mesh plots across the *X* and *Y* axes at several values of *Z* across the bottom half of the cage (the top half of the cage being identical with respect to distance from the cage center). These effectively represent "slices" along *Z* of magnetic field strength in the *X*-*Y* plane, and can be compared to the measured magnetic field in Section VI that use the same coordinates for each plot.

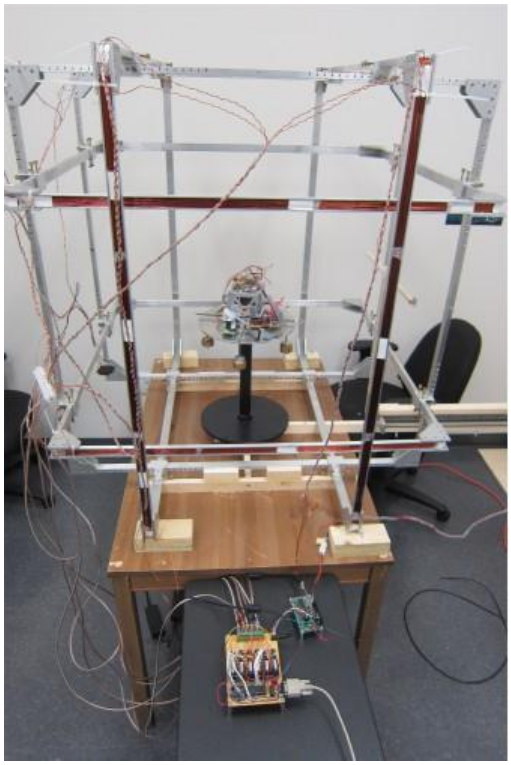

Figure 5 Helmholtz cage with controller and air bearing

III. Mechanical Design

A Helmholtz cage can produce a homogeneous magnetic field region with a desired magnitude relative to all three axes [18]. Helmholtz cages are conventionally circular, however it has been proven in other work [9][10] that square coils can produce a larger homogeneous field area than circular coils of similar dimension, and are also easier to build. This cage design consists of three pairs of coils that are positioned orthogonally to each other. To fit outside the preceding coil's volume, the coils are built in three different side lengths: 38" (0.9652 m), 40" (1.016 m), and 42" (1.0668 m) using standard 1" aluminum u-channels connected in square coils by two corner brackets at each corner. Each coil supports N = 36 turns of 16 AWG magnet wire. In assembled configuration, the coils are

connected together at their crossing points by right-angle connectors machined from rectangular aluminum tube stock, such that the entire structure is self-supporting and does not require a heavy external frame. In order to achieve the required 0.5445 separation ratio for maximum uniformity in all three axes, the spacing between the coils are set to 20.96" (0.5324 m), 21.78" (0.5532 m), and 22.87" (0.5809 m) for the *X*, *Z*, and *Y* axes respectively. If different coil geometries are required, the coils can be adjusted easily by sliding the right-angle connectors to a new position.

To minimize interference from magnetic materials, the cage and structural supports were constructed entirely from aluminum and brass, and a wooden table assembled with nonmagnetic screws is used to support the structure. A desktop computer running MATLAB is used to control the cage and record current and magnetic field telemetry during operation. For characterization, a linear actuator was constructed on one side of the cage to position a MEMS magnetometer at a series of precise locations within the cage volume. The completed cage and air bearing contained within is shown in **Figure 5**.

IV. Electronic Design

The electronic control system for the Helmholtz cage has two main tasks: to drive a calculated amount of current in each coil of wire, and to read the resulting magnetic field using a magnetometer. A block diagram of the controller is shown in **Figure 6**. The current supply is provided by six separate driver channels, each of which can drive up to a rated 25 A of current. Directional current control is provided by two Infineon BTN7960 40A half-bridges, which include integrated shoot-through, overcurrent, and overtemperature protection, connected to a common high-current 12 V supply. The half-bridge outputs are connected to the two ends of each Helmholtz coil so that current can be driven in either direction like that in a solenoid or other inductive load [19]. Each half-bridge is controlled by a high/low side select signal and PWM signal that switches the current output on and off rapidly to minimize transients in the coils. To monitor the average current output at a given time, a Honeywell CSNX25 25A Hall-effect current sensor provides a differential voltage signal proportional to the current flow out of one side of the driver. Control and telemetry processing is implemented on an Atmel ATMega644P AVR 8-bit microcontroller. Each of the six PWM pins on the microcontroller is used to control the current fed to a coil on the cage by disabling both half-bridges on a channel at a time. An additional GPIO pin is used to select the high or low side on each half-bridge, using twelve GPIO pins in total, so that current direction can be controlled by setting one of each pair of half-bridges to high side operation and the other to low side. Six ADC channels on the microcontroller are used to measure the voltage outputs of the six CSNX25 current sensors in real time. The magnetic field produced is measured by a Honeywell HMC5883L MEMS 3-axis magnetometer IC, positioned within the cage by a linear actuator and connected via I^2C bus to the microcontroller. Simple MATLAB functions are used to directly control the cage via RS-232 serial port from a host computer. Preprogrammed byte sequences instruct the coil controller to produce a given PWM, current, or field value within the cage, and also to send back PWM, current, and magnetic field measurements read from the CSNX25 current sensors and the HMC5883L magnetometer. Testing has proven that steady fields of 100 μT can be reached with approximately 2 A of current, which is still well within the capabilities of the driver system.

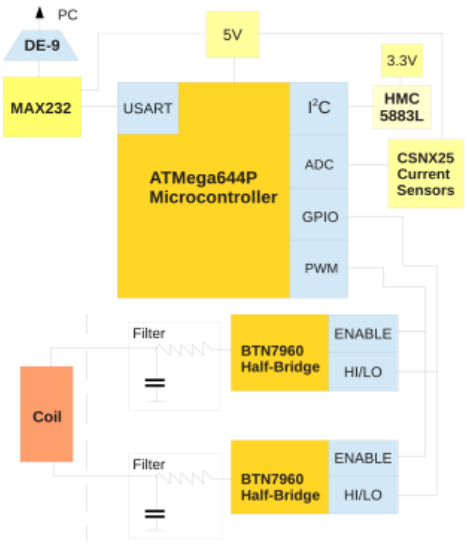

Figure 6 Block diagram of control electronics

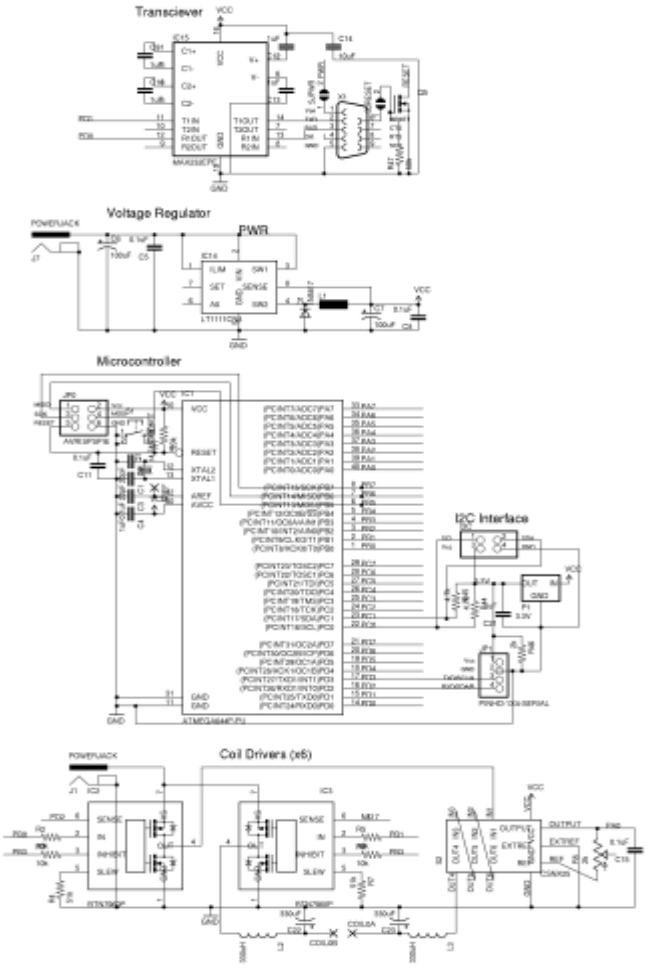

Figure 7 Coil controller schematic

As the PWM frequency available to the driver is constrained to 7.2 kHz by limitations in the half-bridges and microcontroller, it is necessary to filter frequencies down to approximately 700 Hz from the current flow to ensure a consistent magnetic field is produced. A high-current inductor and capacitor on each coil lead are used to form an RLC filter with the coil resistance, in effect increasing the total inductance and capacitance in the coil. A total capacitance of C = 330 μF and inductance of L = 330 μH are used to place the 3dB frequency at $f_{3\mathrm{dB}} = 1/\sqrt{LC} = 482$ Hz and a coil resistance of R = 4 Ω provides a moderate damping ratio of $\zeta = 1/2\mathrm{R}\sqrt{L/C} = 0.125$. The driver circuit with one output channel is shown in **Figure 7**, and a diagram of the complete system formed by the control computer, CubeSat model, coil drivers, linear actuator, and magnetometer is shown in **Figure 8**.

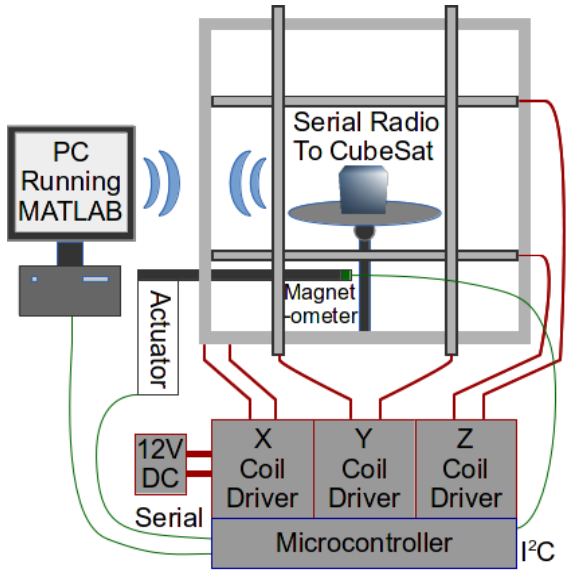

Figure 8 Complete simulator system diagram

V. System Calibration

The resistance in each coil is nominally 4 Ω, but it varies between coils due to the difference in length of the wire windings, and calibration of each channel is needed to ensure consistent current levels. To ensure that repeatable current values are used, the cage was calibrated by measuring current output versus PWM duty cycle (as a signed 8-bit value out of a maximum of 127), **Figure 9** shows the output currents to each coil with respect to the PWM duty cycle of the controller. Duty cycles that are positive denote a current flow in the right-handed direction through the coil, while negative duty cycles denote a current flow in the left-handed direction for intuitive display. It can be seen that the relationship between duty cycle and resulting current is essentially piecewise linear, but exhibits a change in slope at approximately 72 out of 127 due to the response of the circuit. To produce a linear mapping between desired current and PWM duty cycle, a piecewise linear mapping is used, derived from fitting each linear segment in **Figure 9**, and inverting to produce an appropriate PWM duty cycle for a given desired current value in the range $-5 < I_{\mathrm{desired}} < 5$.

While both linear and nonlinear magnetic feedback control laws can be used for coil control based on the current measured by the current sensors [20], the repeatability of magnetic fields produced by a calibrated PWM value is high enough that feedback control is unnecessary.

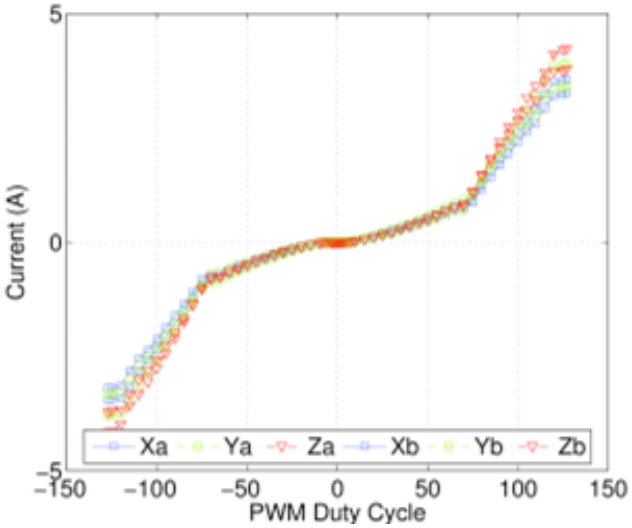

Figure 9 Driver current vs. PWM duty cycle

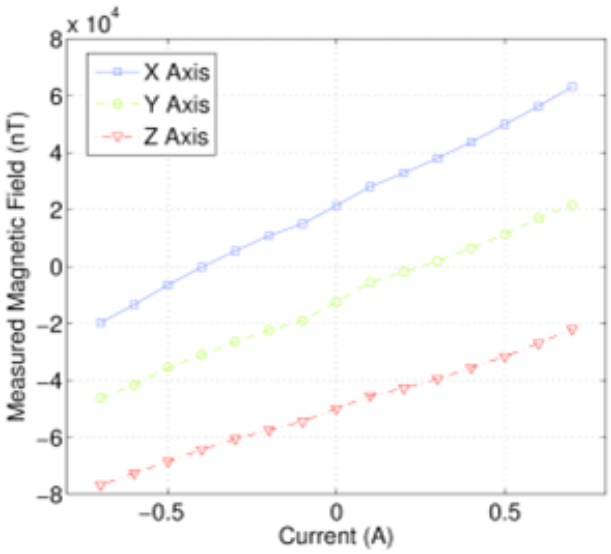

Figure 10 Magnetic field versus current output

To ensure precise control of the magnetic field, magnetometer measurements in three axes for a range of current settings were made at the very center of the cage in the linear region to calibrate the magnetic field output with respect to current. In **Figure 10**, magnetic field in this region is plotted separately with respect to current in each of the X, Y, and Z axes assuming equal current flowing through both coils on a given axis. Linearity of the response is observed to be quite good, with deviation from a linear fit being on the order of ±1 %, although a separate calibration is necessary for each axis to compensate for the difference in field due to the different sizes of the coils. Each of these curves was inverted and used to estimate the desired current for a given magnetic field value for each of the X, Y, and Z axes. In conjunction with the mapping

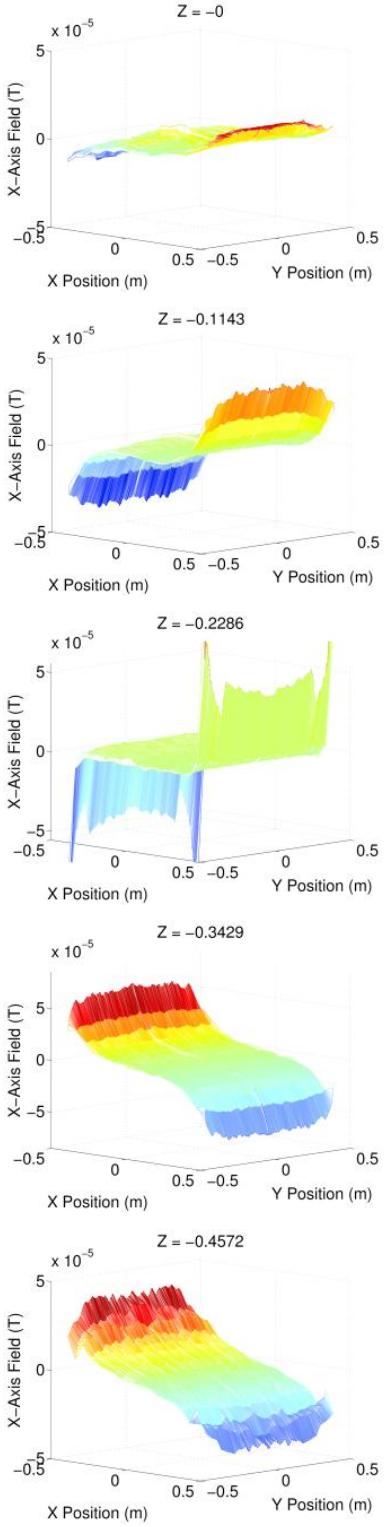

Figure 11 Magnetic field measurements in X direction for lower half-cage

from **Figure 9**, a given magnetic field value can be set with high accuracy and repeatability within the uniform region of the cage. In actual nanosatellite testing, IGRF field values are set within the MATLAB environment by decomposing field vectors into X, Y, and Z directional components and mapping them to PWM values and current directions on the coil controller.

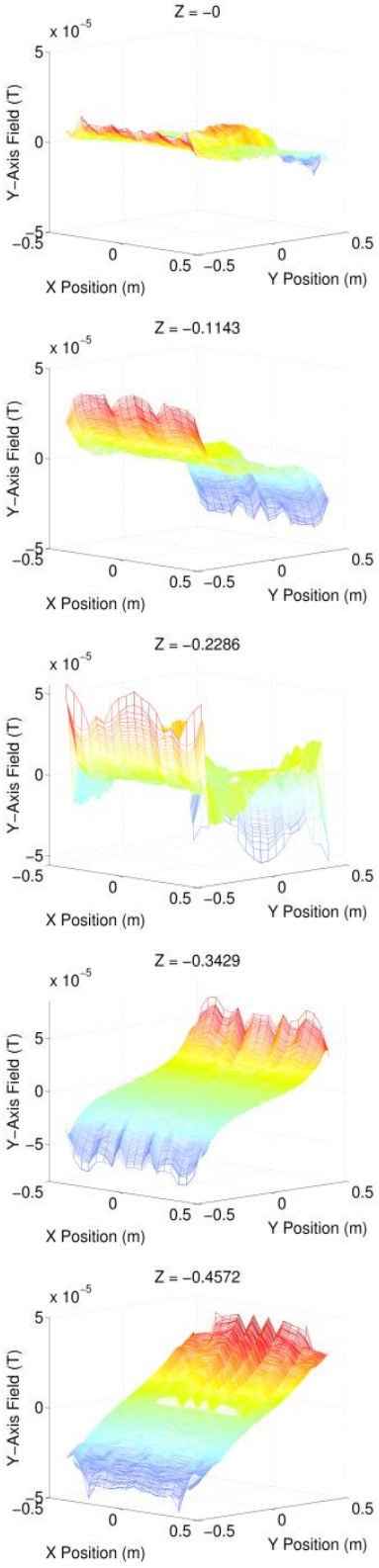

Figure 12 Magnetic field measurements in Y direction for lower half-cage

VI. TESTING RESULTS

To compare the performance of the cage to the numerically calculated model, a series of tests were performed using the linear actuator to obtain a high density of point measurements

along the *Y* direction, while making manual adjustments in the *X* and *Z* directions. To match with the simulation, current values through the coils were manually set to counteract the effect of external magnetic fields as would be done when creating a null-field region, with an additional bias of 1A applied to the *Z*-axis coils. The resulting measurements of *X*, *Y*, and *Z* fields for the bottom half of the cage are shown in **Figure 11**, **Figure 12**, and **Figure 13** for the *X*, *Y*, and *Z* directions respectively. A direct comparison can be made between the simulation results in **Figure 2**, **Figure 3**, and **Figure 4** and the measured data in **Figure 11**, **Figure 12**, and **Figure 13**, particularly regarding the uniform field region in the center of the cage near zero in all plots. In general, there is good agreement between the model and measured field values. Measurement averaging produces reasonable results, though some noise and variation is still present. A nearly-cubic uniform field region spanning nearly 0.4 m on a side with approximately 7 % uniformity is evident in the measurements, indicating that a 3U CubeSat can be tested within this region. The specifications for the completed magnetic simulator are given in **TABLE III**. Also, as a means of performance evaluation, a comparison is shown in **TABLE II** of the magnetic field parameters that were used and estimated for numerical simulations and those that were actually obtained through field measurements in the completed cage.

TABLE I Helmholtz cage design specifications

	Value	Unit
Field Range in Uniform Region	200000	nT
Control Range	200000	nT
Control Resolution	400	nT
X Coil Dimensions	0.965	m
X Coil Resistance	2	Ω
Y Coil Dimensions	1.016	m
Y Coil Resistance	2.2	Ω
Z Coil Dimensions	1.067	m
Z Coil Resistance	2.4	Ω
Total Cage Mass	32	kg
Nominal Voltage Input	12	V
Maximum Current Input	16	A

TABLE II Helmholtz cage simulated and measured performance

	Sim. Value	Meas. Value	Unit
Uniform Field Dimension	0.40	0.37	m
Field Uniformity	2	7	%
Accuracy in Unif. Region	1	2	%
Angular Accuracy	1	5	°

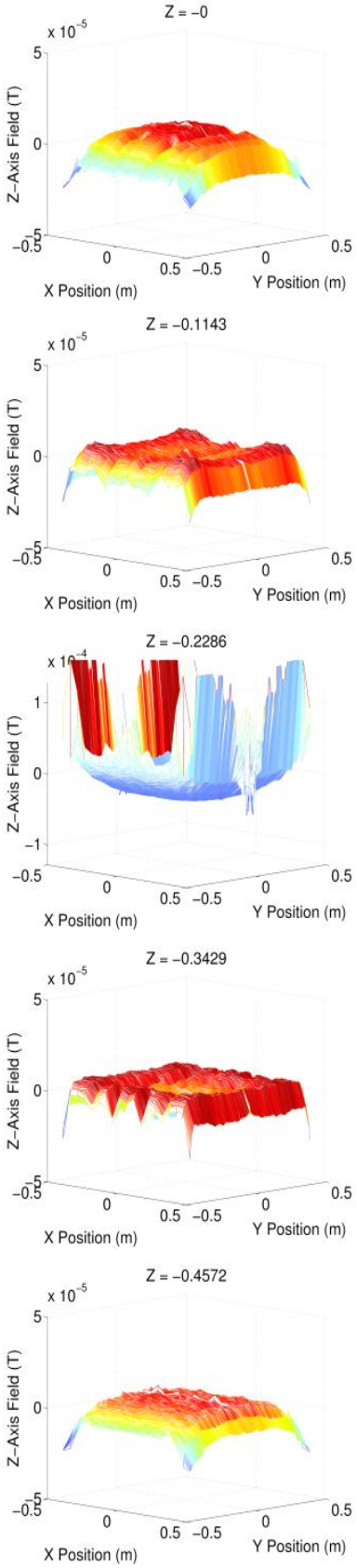

Figure 13 Magnetic field measurements in Z direction for lower half-cage

VII. Conclusion

We have described the development and validation of a laboratory magnetic field simulator that can provide an arbitrarily-oriented magnetic field within a uniform region. The measured field values compare well with numerical results, a suitably large uniform field region is available for testing of up to 3U CubeSats, and calibration of the coils and driver system allows repeatable magnetic fields to be generated under computer control. This system will be used to test nanosatellite magnetic attitude control system hardware for the next generation of research nanosatellites, and due to the use of commonly available components, the design is flexible and inexpensive enough for use in a variety of magnetic research applications.

Acknowledgments

The authors would like to acknowledge the contributions of Houman Hakima and Pablo Saldarriaga to the design and construction of the magnetic field simulator, and the work of Thomas Wright in testing and calibration of the system. The research and development for this facility was made possible by a grant from the MITACS Elevate Program in Canada.

References

[1] X.-W. Zhou, C. T. Russell and G. Le, "Comparison of observed and model magnetic fields at high altitudes above the polar cap: Polar initial results", Geophysical Research Letters, Vol. 24, No. 12, 1997, pp 1451-1454. CrossRef

[2] MacIntyre Electronic Design Associates (MEDA), "HCS01CL with gradient coils operation and maintenance manual", 2007.

[3] K. Grossekatthoefer and C. Raschke, "Support of ACS development and test by dynamic simulation models", 8th IAA Symposium on Small Satellites for Earth Observation, 2011.

[4] F. M. Poppenk, R. Amini, G. F. Brouwer, "Design and application of a Helmholtz cage for testing nano-satellites", 6th International Symposium on Environmental Testing for Space Programmes, Noordwijk, The Netherlands, 2007.

[5] A. Klesh, S. Seagraves, M. Bennett, D. Boone, H. Bahcivan, J. Cutler, "Dynamically driven helmholtz cage for experimental magnetic attitude determination", AAS/AIAA Astrodynamics Specialist Conference, Pittsburgh, PA, 2009.

[6] B. Asokan, "Development of an in orbit simulator for nanosatellites", Master of Science Thesis at Lulea University of Technology, 2012.

[7] M. Pastena, L. Sorrentino, and M. Grassi, "Design and validation of the university of naples space magnetic field simulator (SMAFIS)", Journal of the Institute of Environmental Sciences and Technology Vol. 44, No. 1, 2001, pp. 3342.

[8] M. R. Brewer, "CubeSat attitude determination and helmholtz cage design", Master of Science Thesis at Air Force Institute of Technology, 2012.

[9] F. Piergentili, G. P. Candini, and M. Zannoni, "Design, manufacturing, and test of a real-time, three-axis magnetic field simulator" , IEEE Transactions on Aerospace and Electronics Systems, Vol. 47, No. 2, 2011, pp. 1369-1379. CrossRef

[10] Pastena, M. and Grassi, M., "Optimum design of a three-axis magnetic field simulator", IEEE Transactions on Aerospace and Electronics Systems, Vol.38, No. 2, 2002, pp. 488-501. CrossRef

[11] K. P. Ryan, "Experimental testing of the accuracy of attitude determination solutions for a spin stabilized spacecraft", Master of Science Thesis, Utah State University, 2011.

[12] G. Grandi, and M. Landini, "Magnetic-field transducer based on closed loop operation of magnetic sensors", IEEE Transactions on Industrial Electronics, Vol. 53, No. 3, 2006, pp. 880-885. CrossRef

[13] F. te Hennepe, B. T. C. Zandbergen, and R. J. Hamann, "Simulation of the attitude behaviour and available power profile of the Delfi-c3 spacecraft with application of the opsim platform", 1st CEAS European Air and Space Conference, 2007.

[14] N. Sugimura, K. Fukuda, Y. Tomioka, M. Fukuyama, Y. Sakamoto, T. Kuwahara, T. Fukuhara, K. Yoshida, Y. Takahashi, "Ground test of attitude control system for micro satellite RISING-2", 2012 IEEE/SICE International Symposium on System Integration (SII), Japan, December 2012. CrossRef

[15] T. T. Li, "Tri-axial square Helmholtz coil for neutron EDM experiment", www.phy.cuhk.edu.hk, 2004.

[16] William M. Frix, George G. Karady, Brian A. Venetz, "Comparison of calibration system for magnetic field measurement equipment", IEEE Transactions on Power Delivery, Vol. 9, No. 1, January 1994. CrossRef

[17] W.-S. Lee, W.-I. Son, K.-S. Oh, and J.-W. Yu, "Contactless energy transfer systems using antiparallel resonant loops", IEEE Transactions on Industrial Electronics, Vol. 60, No. 1, 2013, pp. 350-359. CrossRef

[18] S. R. Trout, "Use of Helmholtz coils for magnetic measurements", IEEE Transactions on Magnetics, Vol. 24, No. 4, 1988, pp. 2108-2111. CrossRef

[19] F. Van der Pijl, P. Bauer, M. Castilla, "Control method for wireless inductive energy transfer systems with relatively large air gap", IEEE Transactions on Industrial Electronics, Vol. 60, No. 1, 2013, pp. 382-388. CrossRef

[20] M.-Y. Chen, T.-B. Lin, S.-K. Hung, L.-C. Fu, "Design and experiment of a macro-micro planar maglev positioning system", IEEE Transactions on Industrial Electronics, Vol. 59, No. 11, 2012, pp. 4128-4139. CrossRef